

## BEHAVIOR OF RESIDUAL SALTWATER IN A SUBSURFACE DAM OF SALTWATER INTRUSION PROTECTION TYPE

By

Kei NAKAGAWA

Kagoshima University, 1-21-24 Korimoto, Kagoshima 890-0065, Japan

Kazuro MOMII

Kagoshima University, 1-21-24 Korimoto, Kagoshima 890-0065, Japan

and

Ippei UCHIDA

Graduate School of Kagoshima University, 1-21-24 Korimoto, Kagoshima 890-0065, Japan

### SYNOPSIS

On islands and peninsulas, water shortage frequently takes place due to the absence of geological conditions suitable for construction sites of surface dams. Therefore, several subsurface dam projects are planned or have already been constructed to meet the water demand. A cut-off wall for preventing saltwater intrusion is usually built in coastal areas. After dam construction, investigations of the movement and the removal of residual saltwater in the storage area are often needed. However, because of difficulties in monitoring, estimation of its behavior below ground is usually not carried out. In this study, experimental and numerical studies were performed to understand the fundamental phenomena of saltwater movement after dam construction. Experimental results demonstrated that residual saltwater in the storage area was gradually flushed out under the condition of freshwater discharge over the cut-off wall. Numerical results showed that circulation flow was created in the residual saltwater region after installation of the cut-off wall. The amount of residual saltwater in the storage area will naturally attenuated because new saltwater from the sea is not supplied. Consequently, residual saltwater was gradually transported with the freshwater flow from the inland area. Therefore, countermeasures to remove residual saltwater are not necessary if the dam can be controlled so as to maintain overflow condition of the freshwater.

### INTRODUCTION

It is difficult to develop surface water supplies on islands and peninsulas. The development of groundwater resources by subsurface dams, however, is possible in such regions (1). A subsurface dam consists of a cut-off wall that is constructed to prevent saltwater intrusion and facilitates stable use and control of groundwater ((2) and (3)).

When a subsurface dam is constructed in a coastal aquifer, it should be designed to prevent saltwater intrusion. Numerical simulations can be used to reproduce the situation of saltwater intrusion, and to understand characteristics of freshwater and saltwater flow. It is also important to examine movement of residual saltwater in the storage area of a dam before its construction. Many experimental and numerical studies on saltwater intrusion have been conducted (4). However, the details of residual saltwater have not been examined (see e.g. (5)). In this study, laboratory experiments and numerical simulations were conducted to understand more clearly the basic properties of residual saltwater after construction of a subsurface dam.

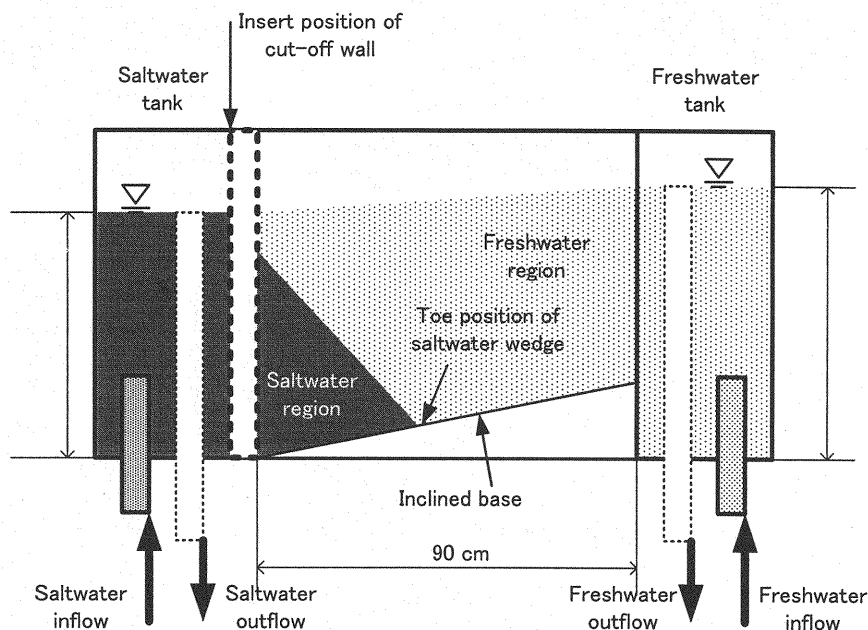


Figure 1 Experimental set-up

## LABORATORY EXPERIMENT

### *Experimental setup and procedure*

Figure 1 shows the experimental set-up including a box (64 cm x 90 cm x 10 cm) filled with sand (particle size 0.05 cm). Beneath the sand, an impermeable layer with a small inclination ( $11^\circ$ ) was installed. The left side of the sand box was filled with saltwater of specific gravity 1.025 (electric conductivity  $54.3 \text{ mS cm}^{-1}$ ) and the water level was set to  $h_s=40 \text{ cm}$ . This saltwater tank is as a simulation of seaside. Saltwater was colored by New Coccin, Acid Red 18 made by Kiriya Chemical Co. Ltd. The right side of the sand box was filled with tap water indicating the freshwater with a water level set to  $h_f=41.5 \text{ cm}$ . The saltwater intrusion experiment started after a cut-off wall located between the saltwater tank and the sand box was removed. This 40.3 cm high cut-off wall ( $h_0$ ) was inserted again, when the saltwater intrusion had reached a steady state. The situation of the saltwater plume intruding the sand aquifer at constant time intervals was photographed by a digital camera. To confirm the exact intrusion position, the toe position of saltwater wedge on the basement was recorded.

### *Experimental results and discussion*

Figure 2 shows change of the toe position of saltwater wedge on the inclined axis (Fig. 1). After 15 hours, the saltwater intrusion reached steady state and the toe position did not proceed further. Figure 3(a) shows digital photos of the steady state of saltwater intrusion. The black part is the saltwater region and the dashed line denotes the observed sharp interface between freshwater and saltwater. At steady state, the freshwater flows from the freshwater tank to the saltwater tank. The saltwater flow towards the freshwater region with a slow velocity and then it dilutes and returns to the saltwater tank in a mixing zone of freshwater and saltwater. By means of this circulation flow, inflow and outflow of saltwater are kept in equilibrium and show a steady state as in Fig. 3(a).

Figures 3(b) and 3(c) show the situation 4 hours and 3 days, respectively, after inserting the cut-off wall. The height of the wall  $h_0$  was kept lower than the freshwater level  $h_f$  and higher than the saltwater level  $h_s$  ( $h_s < h_0 < h_f$ ). Freshwater discharge could occur over the wall. Therefore, just after the wall was inserted, the pressure balance collapsed and deformation of the saltwater plume occurred. With this deformation, the toe position of the saltwater wedge proceeded up on the slope axis. Figure 3(b) shows a photograph when the peak of the toe position is reached. After this, saltwater was transported to the saltwater tank by the

freshwater flow and then saltwater plume decreased. Progress and decline of the saltwater on the slope axis can also be seen in Figure 2. Consequently, the residual saltwater in the storage area is gradually flushed out under the condition of freshwater discharge passing over the cut-off wall. Due to the wall, the supply of saltwater to the aquifer was stopped.

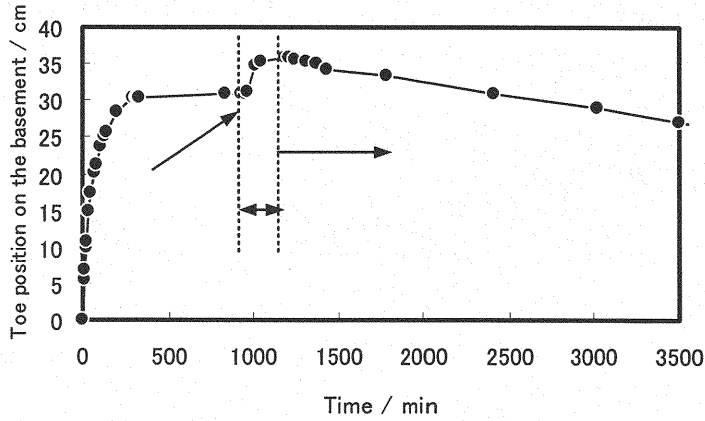


Figure 2 Temporal changes in the toe position of saltwater wedge on the basement

## NUMERICAL SIMULATION

### Basic equations

The following set of equations was applied for the numerical calculations (4):

#### Equation of unsaturated-saturated flow

$$(C_w + \alpha_0 S_s) \frac{\partial h}{\partial t} = -\frac{\partial u}{\partial x} - \frac{\partial v}{\partial y}, \quad u = -k \frac{\partial h}{\partial x}, \quad v = -k \left( \frac{\partial h}{\partial y} + \frac{\rho}{\rho_f} \right) \quad (1)$$

#### Equation of mass conservation (Transport equation)

$$\frac{\partial c}{\partial t} + u' \frac{\partial c}{\partial x} + v' \frac{\partial c}{\partial y} = \frac{1}{\theta} \frac{\partial}{\partial x} \left( \theta D_{xx} \frac{\partial c}{\partial x} + \theta D_{xy} \frac{\partial c}{\partial y} \right) + \frac{1}{\theta} \frac{\partial}{\partial y} \left( \theta D_{yy} \frac{\partial c}{\partial y} + \theta D_{yx} \frac{\partial c}{\partial x} \right) \quad (2)$$

where  $t$  is time,  $h(x, y, t)$  is the piezometric head at the location of  $(x, y)$ ,  $k$  is the hydraulic conductivity,  $u$  and  $v$  are the velocity components in the  $x$  and  $y$  directions which are calculated by Darcy's law,  $u'$  and  $v'$  are the pore velocities calculated as  $u' = u/\theta$ ,  $v' = v/\theta$ ,  $\theta$  is volumetric water content,  $\rho$  is the fluid density,  $\rho_f$  and  $\rho_s$  are the density of freshwater and saltwater, respectively,  $C_w = d\theta/dh$  is the specific moisture capacity for unsaturated conditions,  $S_s$  is the specific storage coefficient,  $\alpha_0$  is a dummy number which takes 0 in an unsaturated condition and 1 in a saturated condition.  $c$  is saltwater concentration coefficient,  $D_{xx}$ ,  $D_{xy}$ ,  $D_{yx}$  and  $D_{yy}$  are dispersion coefficients.

The dispersion coefficients, which are dependent on the velocity, are represented as follows (6):

$$\begin{aligned} \theta D_{xx} &= \frac{\alpha_L u^2}{V} + \frac{\alpha_T v^2}{V} + \theta D_M, \quad \theta D_{yy} = \frac{\alpha_T u^2}{V} + \frac{\alpha_L v^2}{V} + \theta D_M, \\ \theta D_{xy} &= \theta D_{yx} = \frac{(\alpha_L - \alpha_T)uv}{V} \end{aligned} \quad (3)$$

where  $\alpha_L$  and  $\alpha_T$  are the microscopic dispersivity for longitudinal and transverse directions related to the sand particle diameter,  $V = \sqrt{u^2 + v^2}$ , and  $D_M$  is the fluid molecular diffusion coefficient.

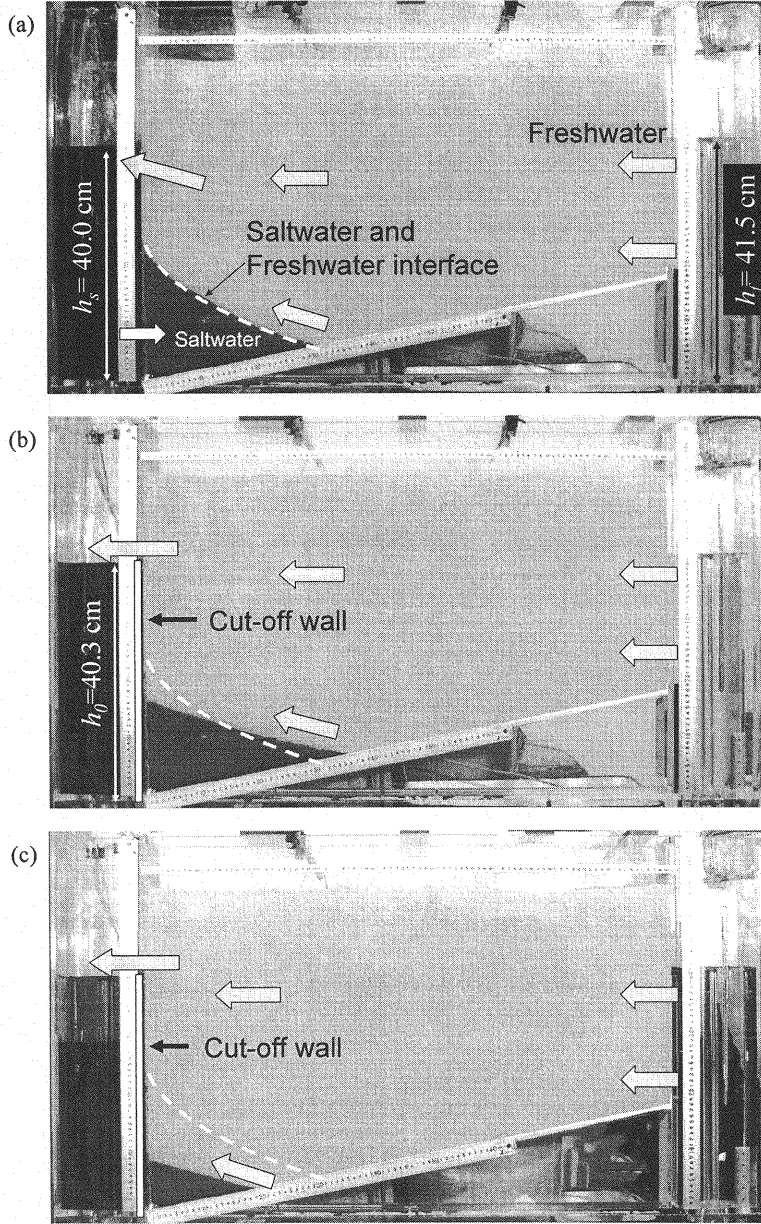


Figure 3 Saltwater plume movements at the steady state and after the insertion of the cut-off wall, (a) Steady state (950 minutes), (b) 4 hours after the wall inserted, and (c) 3 days after the wall inserted

The saltwater concentration  $c(x, y, t)$  in eq.2 is related to the change in the saltwater density through:

$$c(x, y, t) = \frac{100[\rho(x, y, t) - \rho_f]}{(\rho_s - \rho_f)} \quad (4)$$

It is necessary to resolve the relationship  $h$  (negative pressure head) .vs.  $\theta$  (volumetric water content) and  $k_s$  (ratio of saturated hydraulic conductivity) .vs.  $k$  (unsaturated hydraulic conductivity) and to calculate

specific moisture capacity  $C_w$  representing unsaturated characteristics of the aquifer, in order to carry out the numerical simulation including the unsaturated zone. Consequently, in this paper, the unsaturated values were obtained from the theoretical formula of van Genuchten (eq.5) (7).

$$S_0 = \frac{\theta - \theta_r}{\theta_s - \theta_r}, \quad S_e = \left[ \frac{1}{1 + (\alpha |h|)^n} \right]^m$$

$$k_r = S_0^{1/2} \left\{ 1 - \left( 1 - S_e^{1/m} \right)^m \right\}^2$$

$$C_w = \frac{\alpha m (\theta_s - \theta) S_e^{1/m} (1 - S_e^{1/m})^m}{1 - m} \quad (5)$$

where  $\theta_r$  is the residual water content,  $\theta_s$  is the saturated water content and  $\alpha$ ,  $m$  and  $n$  are the coefficients of the van Genuchten formula.

Table 1 Simulation conditions for laboratory experiment

Hydraulic conductivity $k$ (cm s <sup>-1</sup> )	$1.55 \times 10^{-1}$
Longitudinal dispersivity $\alpha_L$ (cm)	0.07
Transversal dispersivity $\alpha_T$ (cm)	0.007
Grid size in $x$ direction $\Delta x$ (cm)	0.5
Grid size in $y$ direction $\Delta y$ (cm)	0.5
Unsaturated flow property for van Genuchten model	
$\theta_s$	0.474
$\theta_r$	0.0492
$\alpha$ (cm <sup>-1</sup> )	0.0829
$n$	5.74

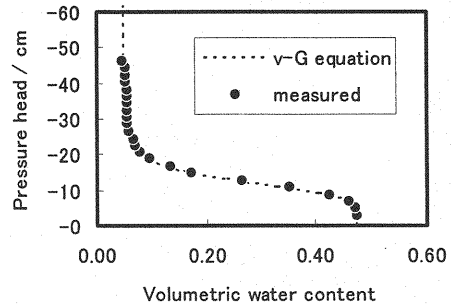


Figure 4 Soil water characteristic curves for sand used in the experiment

#### Numerical simulation procedure and conditions

In the numerical simulation, successive over relaxation (SOR) method was used to solve eq.1 and the method of characteristics (MOC) was used to solve eq.2 (8). The simulation area is 90 cm x 55 cm for  $x$  x  $y$  directions, respectively. Finite difference grid interval was set to 0.5 cm for both  $x$  and  $y$  directions.

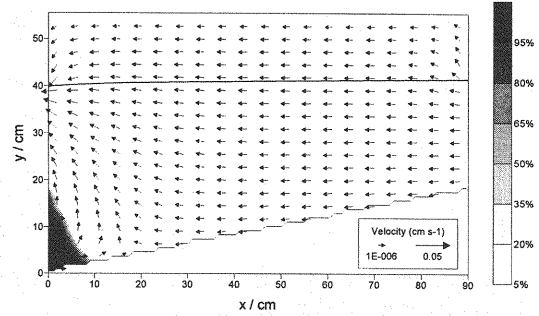
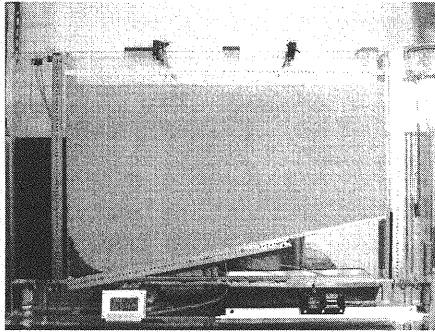
The boundary condition for concentration at the interface between the saltwater tank and sand box was set as follows: for flow out to the sand box (out to the numerical area), the concentration gradient,  $\partial c / \partial x$ , was set to zero, for flow in to the sand box (in to the numerical area), the concentration boundary,  $c$ , was set to 100%. A 0% concentration boundary condition was applied for the right side of the sand box (freshwater tank side). Hydraulic conditions for the saltwater tank and freshwater tank sides were hydrostatic pressure conditions. At the bottom of the numerical area, impermeable and zero mass flux boundary conditions were given. At the top soil surface, zero recharge quantity and 0% concentration boundary conditions were set. After the insertion of the cut-off wall, saltwater tank side boundary conditions were changed to be impermeable and zero mass flux boundary conditions along the cut-off wall. Saltwater and freshwater tank sides of unsaturated zones were set to be zero flux boundary conditions. Above the cut-off wall of saltwater tank side, seepage face was set equal to the pressure head obtained at the previous time step.

#### Numerical simulation results and discussion

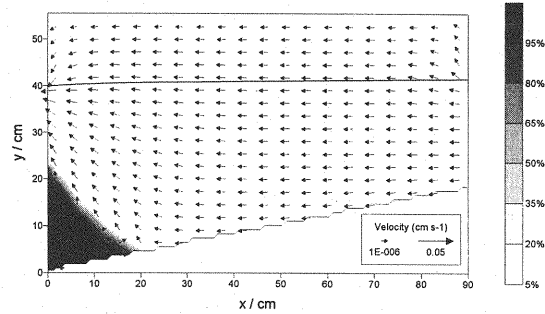
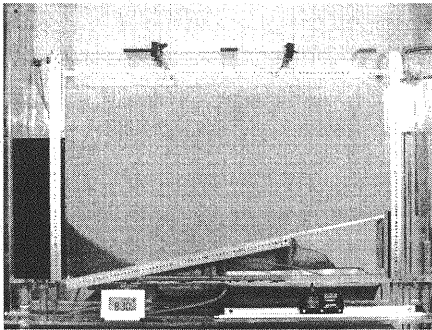
Figure 5 shows the numerical and experimental results of the saltwater intrusion process. The numerical results include saltwater concentration, velocity vector, and groundwater level. The numerical results of the saltwater intrusion process were in good agreement with the experiments, as reported before ((4), (9) and (10)). At first, the intrusion velocity of saltwater was relatively large, and then it gradually decreased, finally reaching a steady state velocity. Intruding saltwater changed the direction in the mixing

zone of freshwater and saltwater and then the saltwater returned to the saltwater tank by freshwater flow. When saltwater intrusion stopped, saltwater inflow and outflows reached equilibrium.

(a)



(b)



(c)

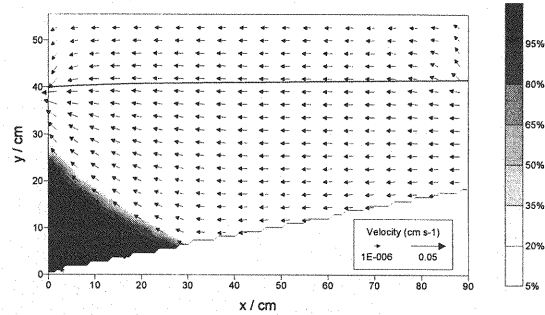
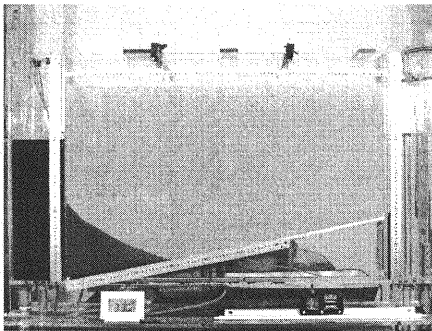


Figure 5 Saltwater intrusion processes of experiment and numerical simulations, (a) 20 min., (b) 80min., and (c) 500 min.

Figure 6 shows the numerical results of saltwater plume movement, which corresponds to Fig. 3. Figure 6(a) shows the steady state for the plume at 950 minutes after intrusion started. Figures 6(b) and 6(c) show the results at 4 hours and 3 days after the cut-off wall was inserted, respectively. The numerical results of saltwater plume movement were in good agreement with the experiments.

Figure 7 shows a close-up view of velocity vectors and saltwater concentration distribution at 4 hours after the wall was inserted. Circulation flow occurred in the saltwater region, just after the wall was inserted. This was due to the fact that the saltwater supply was stopped by the wall as well as outflow to the saltwater tank. The dividing point for saltwater outflow and saltwater circulation is approximately at  $y=19$  cm (Figs.

6(b) and 7). The numerical results show that the saltwater was gradually flushed out by freshwater outflow at the mixing zone (Figure 7). Observations were not clear, however, the numerical results showed mixing zone of freshwater and saltwater extended by the freshwater outflow which had large flux near the cut-off wall (Figure 6(c)).

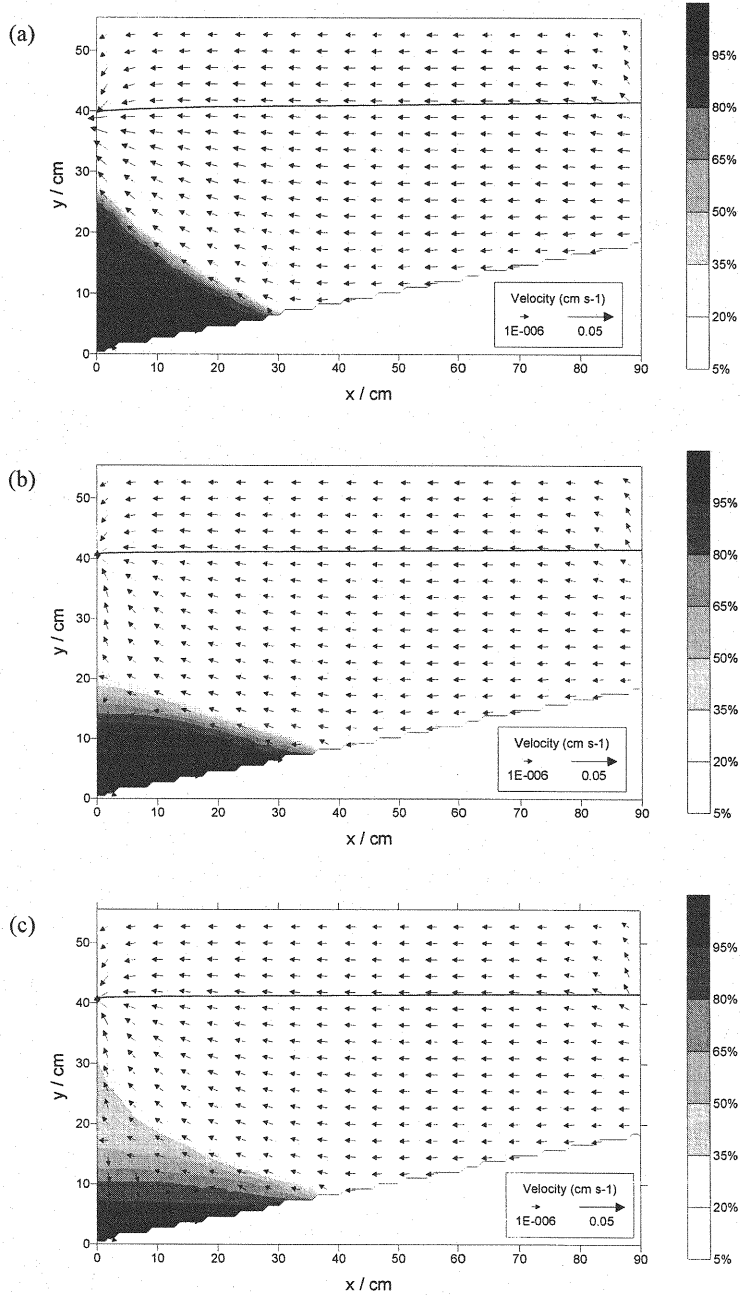


Figure 6 Saltwater plume movements at the steady state and after the insertion of the cut-off wall, (a) Steady state (950 minutes), (b) 4 hours after the insertion of the wall, and (c) 3 days after the insertion of the wall (figures correspond to figures in Fig. 3)

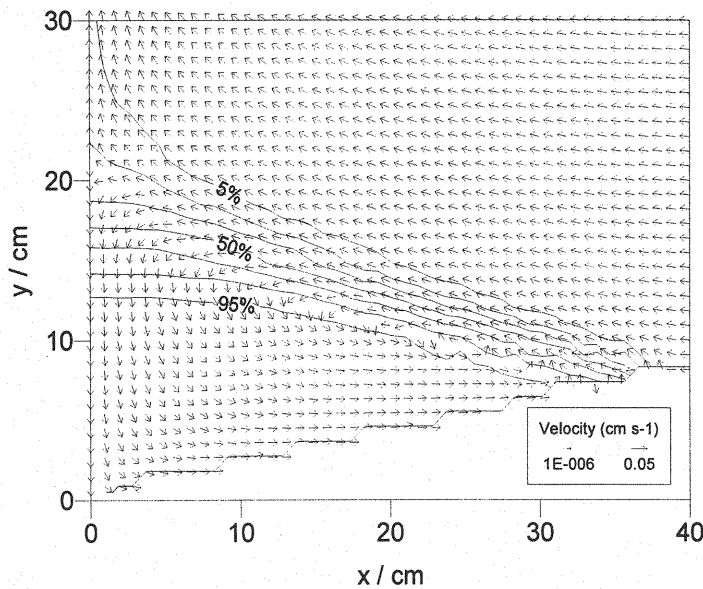


Figure 7 Close view of the velocity vector and saltwater concentration distributions at 4 hours after the insertion of the wall

For the numerical results, during steady state the groundwater level equaled the saltwater level of  $h_s=40$  cm. After the cut-off wall was installed the freshwater level rose to 40.3 cm (height of cut-off wall). Here, the boundary condition along the wall was impermeable condition ( $u=0$ ). This meant that the groundwater level behind the right side of the wall rose and freshwater outflow over the wall was possible. This meant that the groundwater level behind the right side of the wall rose, and it was possible that freshwater flow over the wall. This phenomenon was treated as a new seepage face boundary condition. Fresh water could flow out through this seepage face to the saltwater tank. In order to satisfy the conditions of continuity, the freshwater discharge flux had to be made larger as calculation continues until its quantity equals the inflow quantity of freshwater from the freshwater tank side.

The numerical and experimental results for the attenuation of the saltwater plume did not coincide perfectly. The height of the cut-off wall was 40.3 cm in the experimental conditions. But it was 40.0 cm in the numerical condition, due to the grid interval ( $\Delta y=0.5$  cm). The seepage position was determined by previous time step results of pressure head. In the calculations, this seepage position was actually only one grid step above the wall. These properties affected the calculated quantity of freshwater outflow.

As mentioned above, the numerical results of saltwater wedge movement and attenuation of saltwater plume showed relatively good agreement with experiments. To improve the precision of numerical simulation, the numerical conditions and hydraulic parameters such as dispersivity and hydraulic conductivities should be sufficiently examined.

## CONCLUSIONS

We conducted laboratory experiments and numerical simulations to investigate the movement of residual saltwater in the storage area after a subsurface dam construction. Under the conditions of freshwater discharge passing over the cut-off wall, toe position of the saltwater wedge advanced on the sloping axis due to density effect and then its volume gradually became smaller. As mentioned previously, a measure to remove residual saltwater after a dam construction appears not to be necessary. A prerequisite for this is an outflow over the cut-off wall. Our investigations are not for a real-scale subsurface dam. However, the importance of providing numerical and experimental results is to obtain basic knowledge of the freshwater and saltwater movement before and after a cut-off wall is constructed. We did not observe a complete attenuated saltwater plume. However, in this paper we focused mainly on a continued fresh water outflow and the followings saltwater drainage.

The velocity vector distribution from numerical simulation showed that circulation flow takes place in the saltwater plume region after the cut-off wall was inserted and then outside of the plume was washed out by the freshwater flow toward to the saltwater tank side. The present numerical simulation can reproduce the



process of saltwater intrusion with high accuracy as shown in previous investigations ((4), (9) and (10)). It revealed a close agreement with the toe position of the saltwater wedge and the attenuation of saltwater plume. In order to improve the precision of numerical simulations, more attention should be focused on hydraulic parameters such as dispersivity and hydraulic conductivity as well as simulation conditions.

#### ACKNOWLEDGMENTS

We thank Professor Tosao Hosokawa of Kyusyu Sangyou University for helpful comments. We also thank Professor Ronny Berndtsson of Lund University for giving constructive comments on this manuscript.

#### REFERENCES

1. Land and Water Bureau, Ministry of Land, Infrastructure and Transport: *Water Resources in Japan*, p.166, 2001.
2. Sugahara, T.: Artificial Ground Water, *Tsuchi-to-Kiso*, Vol.41, No.1, pp.19-24, 1993
3. Hasegawa, T.: Underground Dam, *Tsuchi-to-Kiso*, Vol.42, No.3, pp.67-68, 1994.
4. Jinno, K. eds.: *Numerical Analysis of Mass Transport in Groundwater*, Kyushu University Press, pp.73-99, 2001.
5. Nakagawa, K., Hosokawa, T., Jinno, K. and Tajiri, K.: Evaluation for the Replacement of the Saltwater Left After the Subsurface Dam Construction, *Proceedings of Annual Conference of the Japan Society of Civil Engineers*, Vol.51, pp.320-321, 1996.
6. Huyakorn, P. S. and Pinder, G. F.: *Computation method in subsurface flow*, Academic Press, New York, 1983.
7. van Genuchten, M.T.: A closed-form equation for predicting the hydraulic conductivity of unsaturated soils, *Soil Science Society of America Journal*, Vol.44, No.5, pp.892-898, 1980.
8. Sato, K. and Iwasa, K. eds.: *Groundwater Hydraulics*, Springer-Verlag, p.204, 2004.
9. Nakagawa, K., Hosokawa, T., Iwamitsu, K., Jinno, K. and Hiroshiro, Y.: Behavior of Fresh and Salt Groundwater in a Sandy Coastal Aquifer under the Beach Erosion Controlling Pipe Drains, *Journal of Hydrosience and Hydraulic Engineering*, Vol.20, No.1, pp.71-82, 2002.
10. Nakagawa, K., Jinno, K., Hosokawa, T. and Iwamitsu, K.: Numerical study on saltwater intrusion in a heterogeneous stratified aquifer, *Journal of the Faculty of Agriculture Kyushu University*, Vol. 45, No.1, pp.317-323, 2000.

#### APPENDIX-NOTATION

The following symbols are used in this paper:

$c$	= concentration of saltwater;
$C_w$	= specific moisture capacity;
$D_M$	= fluid molecular diffusion coefficient;
$D_{xx}, D_{yy}, D_{xy}, D_{yx}$	= dispersion coefficient;
$h$	= piezometric head;
$h_f$	= water level of freshwater tank;
$h_s$	= water level of saltwater tank;
$h_0$	= height of cut-off wall;
$k$	= hydraulic conductivity;
$k_s$	= saturated hydraulic conductivity;
$S_S$	= specific storage coefficient;
$t$	= time;
$u, v$	= Darcy's velocity for $x$ and $y$ directions;
$u', v'$	= pore water velocity for $x$ and $y$ directions;
$V$	= pore water velocity for flow direction;
$\alpha, m$ and $n$	= coefficients of van Genuchten formula;
$\alpha_L, \alpha_T$	= microscopic dispersivity for longitudinal and transverse directions;
$\alpha_0$	= dummy number that takes 0 in unsaturated condition and 1 in saturated condition;
$\theta$	= volumetric water content;
$\theta_r$	= residual water content;
$\theta_s$	= saturated water content; and
$\rho, \rho_f$ and $\rho_s$	= density of fluid, density of fresh water and density of saltwater.